solutions since they correspond to an objective function with an even smaller value, i.e., $z(\mathbf{r}_1, r_2) = -10$. Nevertheless, this is evidently not the last case. We can, furthermore, have the better but not best or optimum solutions as follows: $\mathbf{r}_1 = (0\ 0\ 0\ 0\ 0\ 0\ 6\ 0\ 0\ 0\ 0\ 0)^T$ and $r_2 = 3, \mathbf{r}_1 = (0\ 0\ 0\ 0\ 0\ 0\ 8\ 0\ 0\ 0\ 0\ 0)^T$ and $r_2 = 4, \mathbf{r}_1 = (0\ 0\ 0\ 0\ 0\ 0\ 10\ 0\ 0\ 0\ 0\ 0)^T$ and $r_2 = 5$, and so on.

V. The Algorithm Correction

The problem exposed in the above example is resolved, and a set of correct IP formulation to implement the transformation is obtained, when (11)–(13) are modified as follows:

$$\max z(\mathbf{r}_1, r_2) = \mathbf{r}_1^T \cdot M_0 + r_2 \cdot (\mathbf{1}^T \cdot M_0 - g - 1) \tag{17}$$

subject to

$$\mathbf{r}_1^T \cdot \Theta_u + r_2 \cdot \mathbf{1}^T \cdot \Theta_u \leq 0 \tag{18}$$
$$\mathbf{r}_1^T \cdot M_0 + r_2(\mathbf{1}^T \cdot M_0 - g - 1) \leq -1 \tag{19}$$
$$\mathbf{r}_1, r_2 \in \mathbb{Z}^+. \tag{20}$$

The reader can verify that the modified formulation can solve the problems with an optimal result $\mathbf{r}_1 = (0\ 0\ 0\ 0\ 0\ 0\ 2\ 0\ 0\ 1\ 0\ 0)^T$ and $r_2 = 1$, which lead to an acceptable constraint

$$(0\quad 2\quad 2\quad 2\quad 0\quad 1\quad 2\quad 0\quad 2\quad 0\quad 0\quad 0) \cdot M \leq (4).$$

VI. Conclusion

The modified IP formulation is proposed, which is proved to be valid under any case to determine the feasibility of a transformation and to derive the corresponding solutions. A maximally permissive and computationally efficient policy will be the research focus of our future work.

References

[1] J. Park and S. A. Reveliotis, "Liveness-enforcing supervision for resource allocation systems with uncontrollable behavior and forbidden states," *IEEE Transa. Robot. Autom.*, vol. 18, no. 2, pp. 234–240, Apr. 2002.

A Scale Stretch Method Based on ICP for 3D Data Registration

Shihui Ying, Jigen Peng, Shaoyi Du, and Hong Qiao

***Abstract*—In this paper, we are concerned with the registration of two 3D data sets with large-scale stretches and noises. First, by incorporating a scale factor into the standard iterative closest point (ICP) algorithm, we formulate the registration into a constraint optimization problem over a 7D nonlinear space. Then, we apply the singular value decomposition (SVD) approach to iteratively solving such optimization problem. Finally, we establish a new ICP algorithm, named Scale-ICP algorithm, for registration of the data sets with isotropic stretches. In order to achieve global convergence for the proposed algorithm, we propose a way to select the initial registrations. To demonstrate the performance and efficiency of the proposed algorithm, we give several comparative experiments between Scale-ICP algorithm and the standard ICP algorithm.**

***Note to Practitioners*—In this paper, we proposed the Scale-ICP algorithm, which is used to deal with the registration between two data sets with scale stretches. In practice, there are a large number of such problems. For example, the registration between the range data sets that have different scanning resolutions determined by the distances from the sensor to the object surfaces. The data sets can be not only image data but also the other measured data, and hence it also can be extended to machining industry besides the computer vision field.**

***Index Terms*—Initial registration, iterative closest point (ICP), large-scale stretch, singular value decomposition (SVD), 3D registration.**

I. Introduction

The data sets registration is a common problem in computer vision and the iterative closest point (ICP) method has been shown a best iterative technique to deal with such a registration problem. Especially in recent years, with the image matching procedure regarded as a registration of two point sets in the position and intensity space [2], [20], [22], the extensive application prospect of ICP method has been emerging increasingly in computer vision. When ICP is applied to the registration between two data sets X and Y in $\mathbb{R}^n$, its goal is to find a transformation $\mathbf{F}$ that best aligns X with Y, starting from an initial guess transformation whose parameters are known. This is done iteratively as follows: pair each point in X to the closest point in Y, and then compute the next transformation by minimizing a certain distance between the paired points.

It has been extensively accepted that the present standard ICP method was proposed independently by Besl and McKay [3], Chen and Medioni [4], and Zhang [23], although the rudiment of ICP may

Manuscript received September 01, 2007; revised October 10, 2007 and December 03, 2007. First published May 27, 2009; current version published July 01, 2009. This paper was recommended for publication by Associate Editor J. Fuh and Editor M. Wang upon evaluation of the reviewers' comments. This work was supported in part by NCET and in part by the National Basic Research Program of China under Grant 2007CB311002.

S. Ying and J. Peng are with the Institute of Information and System Science, Faculty of Science, Xi'an Jiaotong University, Xi'an 710049, China (e-mail: Yingshihui@gmail.com; jgpeng@mail.xjtu.edu.cn).

S. Du is with the Institute of Artificial Intelligence and Robotics, Xi'an Jiaotong University, Xi'an 710049, China (e-mail: dushaoyi@gmail.com).

H. Qiao is with the Key Laboratory of Complex Systems and Intelligent Science, Institute of Automation, Chinese Academy of Sciences, Beijing 100080, China (e-mail: hong.qiao@mail.ia.ac.cn).

Color versions of one or more of the figures in this paper are available online at http://ieeexplore.ieee.org.

Digital Object Identifier 10.1109/TASE.2009.2021337

be traced back to the early 1980s when B. D. Lucas proposed an iterative technique for image registration in [14]. There by now has been a large number of research works devoted to improving ICP method, towards two main directions. The first is to accelerate the algorithm and improve the accuracy as far as possible, assuming that the data sets for registration are rigid. In this direction, there have been presented many improved versions of ICP, such as the hybrid method by Rusinkiewicz and Levoy [19], the SIC-range method by Hügli and his coauthors [10], the manifold method by Krishman and his coauthors [12], the trimmed ICP algorithm by Chetverikov *et al.* [5], the LM algorithm by Fitzgibbon [9], and the picky ICP algorithm by Zinßer *et al.* [24]. The second is to reduce the requirement for the data sets. For example, Feldmar and his coauthors in [7] and [8] studied the registration problem of free form surfaces by incorporating scale ingredients. For overviews on data sets registration using ICP method, we also refer to Pennec and Thirion [15], Sharp *et al.* [20], Pottmann *et al.* [17], [18], Ezra *et al.* [6], Liu [13], Zitová *et al.* [25], and Planitz *et al.* [16].

However, the standard ICP algorithm does not take scale factor into account in the registration problem, while the scale factor always exists in registration. For example, the range data set usually has different scanning resolutions determined by the distances from the sensor to the object surfaces. This requires that the registration algorithms be able to estimate the scaling parameter, as well as the general motion parameters between images. In this paper, we consider the registration problem of 3D data sets where large-scale stretches and noises exist. We modify the standard ICP algorithm by introducing a scale factor s with lower and upper bounds, and then formulate the registration problem into a quadric constraint optimization problem over a 7D nonlinear space. To solve such an optimization problem, we design a fast and accurate iterative procedure based on the singular value decomposition (SVD) technique. For the proposed algorithm, we discuss how to select a "good" initial registration to achieve the global minimum. We also give several comparative experiments to verify that the proposed algorithm is really fast and accurate for the registration problems of 3D data sets with large-scale stretches.

The remainder of this paper is organized as follows. In Section II, we propose a model for registration of two 3D scale data sets. In Section III, a commonly explicit iterative rule based on the standard SVD and the properties of the quadric function is given with the corresponding algorithm following. Moreover, in Section IV, a convergence theorem is claimed that the Scale-ICP algorithm is a locally convergent method, and hence a good initial registration is suggested to achieve the global minimum. Several comparative and practical numerical experiments are implemented in Section V and this paper is concluded and further discussed in Section VI.

II. Problem Description and the Scale-ICP Model

The registration of two 3D data sets $X = \{x_i\}_{i=1}^m$ and $Y = \{y_j\}_{j=1}^n$ with different scales can be stated below.

Problem 1 (Registration of Data Sets With Scale Stretch): Find a rotation $R \in SO(3)$, a translation $T \in \mathbb{R}^3$, and a scale s in a given interval I of $\mathbb{R}^+$ such that the resulted set $s \cdot RX + T$ aligns best with Y.

When ICP method is applied, the above problem can be addressed in two iterative steps.

Step 1) For the current rotation R^k, translation T^k, and scale $s^k \in$ I, search a subset Z^k of Y with the same size as X such that the following objective function is minimized:

$$\varepsilon^k(Z) := \sum_{i=1}^m \|s^k \cdot R^k x_i + T^k - z_i\|^2. \tag{1}$$

Step 2) Fixing the obtained Z^k, search the next rotation R^{k+1}, translation T^{k+1}, and scale $s^{k+1} \in$ I such that the following objective function is minimized:

$$e^k(R, T, s) := \sum_{i=1}^m \|s \cdot Rx_i + T - z_i^k\|^2. \tag{2}$$

The optimization problem (1) can be easily solved using the program function *dsearchn* in Matlab, so we only focus our attention on the problem (2), which is obviously a constraint optimization problem over the 7D nonlinear space $SO(3) \times \mathbb{R}^3 \times$ I. In the next section, we will develop an approach to such an optimization problem.

III. A Fast Scale-ICP Algorithm Based on SVD

In this section, we give an iterative rule for Problem 1. To this end, we eliminate the translation T at Step 2 of ICP for Problem 1 by calibrating the centers of X and Z^k, and so we reduce the optimization problem (2) to an optimization problem with respect to R and s. On the base of this, we employ the SVD technique to get the explicit expressions of the next rotation R^{k+1} and the scale factor s^{k+1}.

A. Compute the Next Translation T^{k+1}

Denote by x_c and z_c^k, the centers of the test data set X and the set Z^k at kth step, namely

$$x_c = \frac{1}{m}\sum_{i=1}^m x_i, \quad z_c^k = \frac{1}{m}\sum_{i=1}^m z_i^k. \tag{3}$$

Then, noticing that $(R^{k+1}, T^{k+1}, s^{k+1})$ is the least square solution of (2), we have

$$T^{k+1} = z_c^k - s^{k+1} \cdot R^{k+1} x_c. \tag{4}$$

B. Compute the Next Rotation R^{k+1} and Scale s^{k+1}

To compute the next rotation R^{k+1} and scale s^{k+1}, we let

$$\tilde{x}_i = x_i - x_c, \quad \tilde{z}_i^k = z_i^k - z_c^k. \tag{5}$$

Then, the problem (2) is equivalently simplified into

$$(R^{k+1}, s^{k+1}) = \arg \min_{R \in SO(3), s \in \mathrm{I}} e^k(R, s) := \sum_{i=1}^m \|s \cdot R\tilde{x}_i - \tilde{z}_i^k\|^2. \tag{6}$$

By the orthogonal property of rotation matrix R, we have

$$e^k(R, s) = \sum_{i=1}^m \left[s^2\langle \tilde{x}_i, \tilde{x}_i\rangle - 2s\langle R\tilde{x}_i, \tilde{z}_i^k\rangle + \langle \tilde{z}_i^k, \tilde{z}_i^k\rangle\right]. \tag{7}$$

That is, $e^k(R, s)$ is a quadric function of $s \in$ I with positive coefficient of quadric term. Hence, if e^k achieves its minimum at (R^{k+1}, s^{k+1}), then s^{k+1} necessarily satisfies the following equality:

$$\frac{\partial}{\partial s} e^k(R, s) = 0. \tag{8}$$

Solving (8), we get that

$$s = \frac{\sum_{i=1}^m \langle R\tilde{x}_i, \tilde{z}_i^k\rangle}{\sum_{i=1}^m \langle \tilde{x}_i, \tilde{x}_i\rangle} \tag{9}$$

which could be the candidate of the next scale s^{k+1}. It should be noted that the s determined by (9) may be out of the range of the interval I. Hence, it is quite necessary to discuss the solution s of (9). For this, we assume $\mathrm{I} = [a, b]$, $a > 0$, without loss of generality.

1) If $s \leq a$(or $\geq b$), the quadric function $e^k(R, s)$ achieves in I its minimum at a (or b). In this case, we set

$$s^{k+1} = a \text{ (or } b). \tag{10}$$

Consequently, minimizing $e^k(R, s)$ is equivalent to maximizing the following function of R over $SO(3)$:

$$F^k(R) = \sum_{i=1}^{m} \langle R\tilde{x}_i, \tilde{z}_i^k \rangle. \tag{11}$$

2) If $a < s < b$, then we set s as the next scale s^{k+1}. Substituting this scale into (6), we get that

$$e^k(R, s) = -s^{k+1} \sum_{i=1}^{m} \langle R\tilde{x}_i, \tilde{z}_i^k \rangle + \sum_{i=1}^{m} \langle \tilde{z}_i^k, \tilde{z}_i^k \rangle. \tag{12}$$

It follows that minimizing $e^k(R, s)$ is also equivalent to maximizing the function of R defined by (11).

The above discussion indicates that in either case 1) or case 2), we can compute the next rotation R^{k+1} by maximizing the same one-variable objective function $F^k(R) = \sum_{i=1}^{m} \langle R\tilde{x}_i, \tilde{z}_i^k \rangle$ other than the bi-variable objective function $e^k(R, s)$. Below, we apply the SVD method to maximizing such one-variable function $F^k(R)$ over the Lie group $SO(3)$.

Let H be the 3×3 matrix defined by $H := \sum_{i=1}^{m} \tilde{x}_i (\tilde{z}_i^k)^T$. According to the singular value decomposition principle [1], [22], there are 3×3 orthogonal matrices U and V and a 3×3 diagonal matrix Λ with non-negative elements such that $H = U \Lambda V$. By [1], we know that, as the maximum point of the function $F^k(R)$, the next rotation R^{k+1} is given by (13)

$$R^{k+1} = \begin{cases} VU^T, & \det(VU^T) = 1 \\ V \begin{pmatrix} 1 & 0 & 0 \\ 0 & 1 & 0 \\ 0 & 0 & -1 \end{pmatrix} U^T, & \det(VU^T) = -1 \end{cases}. \tag{13}$$

Accordingly, setting

$$s^{k+1} = \begin{cases} a, & s \leq a \\ b, & s \geq b \\ \frac{\sum_{i=1}^{m} \langle R^{k+1}\tilde{x}_i, \tilde{z}_i^k \rangle}{\sum_{i=1}^{m} \langle \tilde{x}_i, \tilde{x}_i \rangle}, & a < s < b \end{cases}. \tag{14}$$

We achieve the following algorithm for Problem 1.

Algorithm 1 (Scale-ICP Algorithm):

Step 1) Given two data sets $X = \{x_i\}_{i=1}^m$ and $Y = \{y_j\}_{j=1}^n$.

Step 2) Initialize rotation R^0, translation T^0, scale factor s^0 and precision $\epsilon > 0$.

Step 3) Iteration (Step k).

- Step 3.1) Find the point set $Z^k = \{z_i^k\}_{i=1}^m$ in Y closest to $X = \{x_i\}_{i=1}^m$.
- Step 3.2) Compute R^{k+1} by formula (13).
- Step 3.3) Compute s^{k+1} by formula (14).
- Step 3.4) Compute T^{k+1} by formula (4).

Step 4) Terminating rule

$$\text{Compute } \theta = 1 - \frac{e^{k+1}(R^{k+1}, T^{k+1}, s^{k+1})}{e^k(R^k, T^k, s^k)}$$

- Step 4.1) If $\theta \leq \epsilon$, output the minimum $(R^*, T^*, s^*) = (R^{k+1}, T^{k+1}, s^{k+1})$.
- Step 4.2) Else $k \Leftarrow k + 1$ and goto Step 3.

IV. Initial Registration and Convergence Analysis

In this section, we first prove a local convergence theorem for the Scale-ICP algorithm, which is similar to that of [3]. Then, we discuss how to select a "good" initial registration (R^0, s^0, T^0) to achieve the global minimum.

Theorem 1: The Scale-ICP algorithm converges monotonically to a local minimum.

Proof: Let $X = \{x_i\}_{i=1}^m$ and $Y = \{y_j\}_{j=1}^n$ be two data sets in $\mathbb{R}^3$. Let R^k, T^k, s^k and $Z^k = \{z_i\}_{i=1}^m$ be the rotation matrix, translation, scale, and the closest point set at kth step. Then, the current error is given by

$$\varepsilon^k = \sum_{i=1}^{m} \| s^k \cdot R^k x_i + T^k - z_i^k \|^2 \tag{15}$$

and the next error is given by

$$e^k = \sum_{i=1}^{m} \| s^{k+1} \cdot R^{k+1} x_i + T^{k+1} - z_i^k \|^2. \tag{16}$$

It is easy to check that $e^k \leq \varepsilon^k$, otherwise, we let $R^{k+1} = R^k$, $T^{k+1} = T^k$ and $s^{k+1} = s^k$. Similarly, $\varepsilon^{k+1} \leq e^k$ because of the inequality $\|s^{k+1} \cdot R^{k+1} x_i - z_i^{k+1}\| \leq \|s^{k+1} \cdot R^{k+1} x_i - z_i^k\|$ for all $i = 1, \ldots, m$. Therefore, we have that

$$0 \leq \cdots \leq e^{k+1} \leq \varepsilon^{k+1} \leq e^k \leq \varepsilon^k \leq \cdots \quad \forall k. \tag{17}$$

This indicates that the square error sequence $\{\varepsilon^k\}_{k \geq 1}$ is monotone nonincreasing and lower bounded, and so it follows that the algorithm converges to a minimum value. ■

Like the standard ICP algorithms, the Scale-ICP algorithm is local. In other words, its convergence to the global minimum strongly depends on the initial registration. A common way to achieve the global minimum is to find the minimum of all the local minima [3], [10]. It is clear that in Algorithm 1 the convergence localness is raised from Step 3.1 finding the closest points, since the other optimization (2) is obviously global by the convex theorem [11]. Next, we present a new way of selecting a "good" initial registration (R^0, s^0, T^0) to achieve the global minimum.

It is well known that variability of data sets is able to be described by the covariance matrix whose many properties can be characterized by its eigenvalues and eigenvectors. Given two data sets $X = \{x_i\}_{i=1}^m$ and $Y = \{y_j\}_{j=1}^n$. Their covariance matrices are evaluated, respectively, by $M_X := \sum_{i=1}^{m} (x_i - x_c)(x_i - x_c)^T$ and $M_Y := \sum_{j=1}^{n} (y_j - y_c)(y_j - y_c)^T$, where x_c and y_c stand for the centers of X and Y. Let $\lambda_1 \leq \lambda_2 \leq \lambda_3$ and $\mu_1 \leq \mu_2 \leq \mu_3$ be the eigenvalues of M_X and M_Y, and let p_1, p_2, p_3 and q_1, q_2, q_3 be their normalized eigenvectors correspondingly. From the geometrical meaning, the geometric distributions of X and Y are similar if

$$\alpha - \Delta\alpha \leq \sqrt{\frac{\mu_i}{\lambda_i}} \leq \alpha + \Delta\alpha, \quad i = 1, 2, 3 \tag{18}$$

holds for some small offset $\Delta\alpha$, where $\alpha = 1/3 \sum_{i=1}^{3} \sqrt{\mu_i/\lambda_i}$. So, to achieve the global minimum, we suggest that the initial scale s^0 be selected close to α and the interval I of the scale s be selected as $\left[\min_i \left\{\sqrt{\mu_i/\lambda_i}\right\}, \max_i \left\{\sqrt{\mu_i/\lambda_i}\right\}\right]$. At the same time, since eigenvalues represent the distributions of data set along their corresponding normalized eigenvectors, we suggest that the initial rotation R^0 be selected close to the vector $[q_1, q_2, q_3]\,[p_1, p_2, p_3]^{-1}$ and the initial translation T^0 be selected close to $y_c - x_c$. Here, for the related discussion

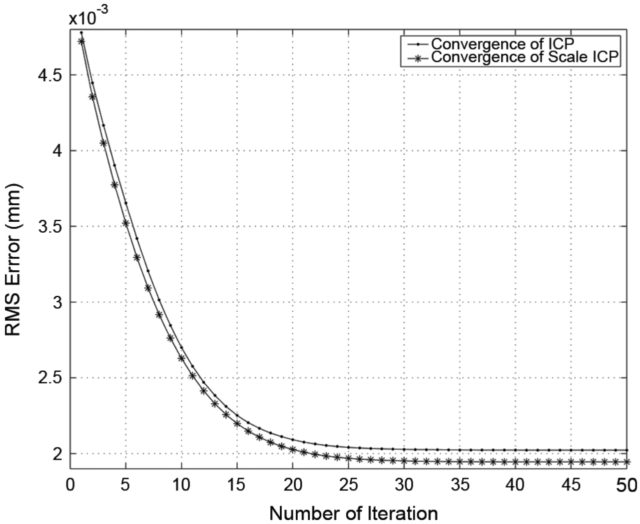

Fig. 1. RMS errors of registration within 50 iterations by two algorithms.

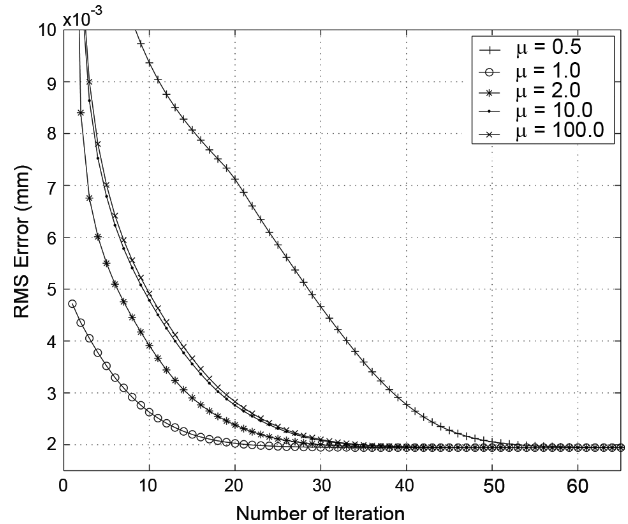

Fig. 2. Portraits of the RMS errors of five registrations.

TABLE I
REGISTRATION RESULT OF ICP AND SCALE-ICP

	ICP	Scale-ICP
Rotation Axis	(-0.0012 0.5668 0.0067)	(-0.0051 0.5654 0.0161)
Rotation Angle	32.4783 degs	32.4112 degs
Translation	(-0.0520 -0.0003 -0.0120)	(-0.0500 0.0014 -0.0108)
Scale	–	0.97998
RMS Error	0.00202 mm	0.00194 mm

on the selection of the initial rotation and initial translation, we refer to [3].

We will follow the above principle to select the initial registration (R^0, s^0, T^0) in simulations of the next section, where the algorithm convergence is really global.

V. NUMERICAL EXPERIMENT

This section is divided into two parts: 1) the comparison between the standard ICP algorithm and Scale-ICP algorithm for the registration of 3D range data sets without scale stretch and 2) the registration between two range data sets with scale stretch, by Scale-ICP algorithm. All programs are written in Matlab6.5 and run by PC with PentiumIV3.0GHz CPU and 512M RAM.

1) Part I: Comparison between the standard ICP algorithm and Scale-ICP algorithm.

In this part, Stanford 3D Scanning Repository[1] is employed to compare the standard ICP algorithm with the Scale-ICP algorithm. As an explanation experiment, we only display and explain the result of registration between bun045 (40097 points) and bun000 (40256 points) of the Stanford Bunny data set [9]. With the precision $\epsilon = 0.001$, the initial rotation axis $(\,-0.0534 \quad 0.4425 \quad -0.0602\,)$ and rotation angle 25.7695°, and the initial translation $(\,-0.0557 \quad 0.0006 \quad -0.0214\,)$, the standard ICP algorithm arrives the optima at the 28th step consuming 33.268 s, while the Scale-ICP algorithm, with the additional initial scale $s^0 = 1.0092$ and the scale interval $\mathrm{I} = [0.9506,\ 1.0923]$, arrives the optima at the 30 step consuming 40.053 s. The comparison results are displayed in Table I and portrayed in Fig. 1.

With the resulted RMS errors displayed in Table I, it is computed that the registration accuracy is improved by $3.844\%(= \mathrm{RMS}_{\mathrm{ICP}} - \mathrm{RMS}_{\mathrm{ScaleICP}}/\mathrm{RMS}_{\mathrm{ICP}} \times 100\%)$ by the Scale-ICP method. Fig. 1 exhibits the accuracy improvement. The numerical results demonstrate that, for registration of the data sets with noises, both algorithms are efficient in the same way, but the Scale-ICP algorithm is able to improve the registration accuracy.

2) Part II: Registration of two range data sets with scale stretch.

To demonstrate the advantage of Scale-ICP algorithm for registrations between two data sets with different scales, we consider the group of registrations between the data set bun045 and each data set generated by multiplying bun000 by some scales μ, respectively. For the sake of the error comparability, we adopt the following modified RMS error

$$\mathrm{RMS} = \frac{1}{\mu}\left(\frac{1}{m}\sum_{i=1}^{m}\|s^*R^*x_i + T^* - z_i^*\|^2\right)^{1/2} \tag{19}$$

where R^*, T^*, and s^* are the iteration terminal rotation, translation and scale, and z_i^* is the closest point to the point $s^*R^*x_i + T^*$. With the precision $\epsilon = 0.001$ and the respective initial registrations with $\mu = 0.5, 1.0, 2.0, 10.0$, and 100.0 (see Table II), we obtain the corresponding numerical results displayed in Table III and portrayed in Figs. 2–4. From Table III, it is seen that: 1) the five terminal RMS errors are all identical, that is, all five iteration sequences approximate to the same value in the given iteration length; 2) the five terminal rotations are all identical, which verifies the fact that the scale stretches introduced by us do not change the rotation stages of data sets; and 3) the five terminal scales s^* are quite close to the actual ones μ, which demonstrates the performance of Scale-ICP algorithm robust to the scale bias. Moreover, that the displayed five translations appear to be different is because the translations occur after the scale stretches. In fact, if every terminal T^* is divided by its corresponding μ, then we can find that the resulted translations are all the same in the given precision. Five RMS error sequences are portrayed in Fig. 2. The initial configurations of the data set bun045 (red) and the data set generated by multiplying bun000 by $\mu = 0.5$ (blue) are portrayed in Figs. 3 and 4 exhibits the configurations of two data sets after registration.

We further consider the group of registrations between the data set dragonStandRight_48 (22092 points) and each data set generated by multiplying dragonStandRight_0 (41841 points), respectively, by the scales $\mu = 0.5,\ 1.0,\ 2.0,\ 10.0$ and 100.0. The corresponding numerical results for $\mu = 0.5$ are portrayed in Figs. 5 and 6.

VI. CONCLUSION AND FURTHER DISCUSSION

In this paper, we addressed ourselves to the registration of two 3D data sets with noises and large-scale stretches. By incorporating a

[1]http://www-graphics.stanford.edu/data/3Dscanrep/.

TABLE II
INITIAL REGISTRATION FOR DATA SETS WITH DIFFERENT SCALES

μ	Rotation Axis	Rotation Angle	Translation	Scale	Scale Boundary
0.5	(-0.0534 0.4425 -0.0602)	25.7695°	(-0.0437 -0.0477 -0.0392)	0.5046	$[0.4753, 0.5461]$
1.0	(-0.0534 0.4425 -0.0602)	25.7695°	(-0.0057 0.0006 -0.0214)	1.0092	$[0.9506, 1.0923]$
2.0	(-0.0534 0.4425 -0.0602)	25.7695°	(-0.0797 0.0972 0.0142)	2.0185	$[1.9013, 2.1845]$
10.0	(-0.0534 0.4425 -0.0602)	25.7695°	(-0.2718 0.8699 0.2993)	10.0924	$[9.5064, 10.9226]$
100.0	(-0.0534 0.4425 -0.0602)	25.7695°	(-2.4337 9.5625 3.5061)	100.9241	$[95.0643, 109.2257]$

TABLE III
RESULTS OF REGISTRATION FOR DATA SETS WITH DIFFERENT SCALES

μ	Rotation Axis	Rotation Angle	Translation	Scale	RMS Error	Loop	Time (s)
0.5	(-0.0051 0.5654 0.0161)	32.4112°	(-0.03003 0.00083 -0.00649)	0.48999	0.00194 mm	61	82.564
1.0	(-0.0051 0.5654 0.0161)	32.4112°	(-0.03503 0.00097 -0.00757)	0.97998	0.00194 mm	30	40.053
2.0	(-0.0051 0.5654 0.0161)	32.4112°	(-0.04003 0.00111 -0.00865)	1.95996	0.00194 mm	39	53.865
10.0	(-0.0051 0.5654 0.0161)	32.4112°	(-0.04504 0.00125 -0.00973)	9.79982	0.00194 mm	43	61.187
100.0	(-0.0051 0.5654 0.0161)	32.4112°	(-0.05004 0.00139 -0.01081)	97.99823	0.00194 mm	43	63.756

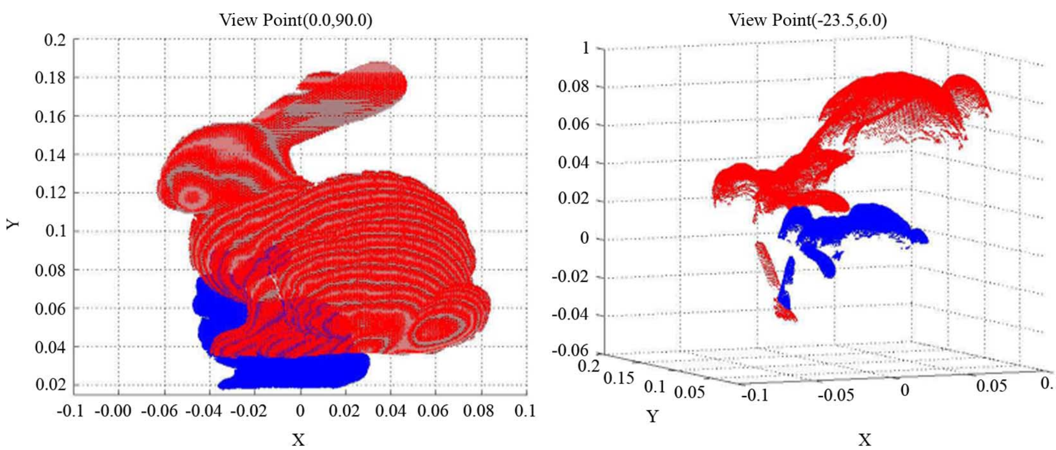

(a) View Point (0.0,90.0) (b) View Point (-23.5,6.0)

Fig. 3. Original configuration of two data sets when $\mu = 0.5$.

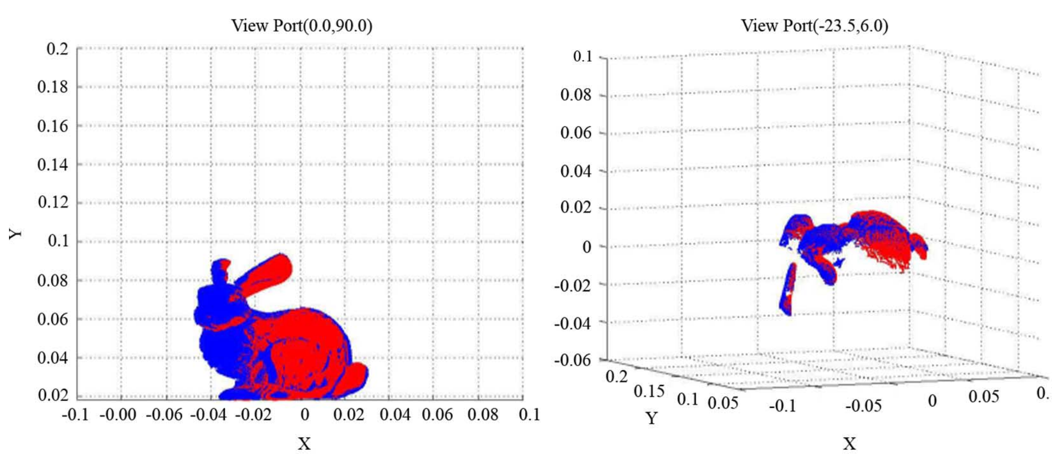

(a) View Point (0.0,90.0) (b) View Point (-23.5,6.0)

Fig. 4. Configurations of two data sets after registration.

scale factor to the standard ICP algorithm, we developed a new ICP algorithm, named Scale-ICP algorithm, whose advantages mainly exist in: 1) for the registration of data sets with the same scale, the presented comparative experiments demonstrated that, without loss of computational efficiency, it is more accurate than the standard ICP algorithms; 2) for the registration of data sets where exist large scales, it can implement registration accurately, while the standard ICP algorithm cannot do that; and 3) its iterations are of closed form. In the authors' opinion, the proposed Scale-ICP algorithm is distinguished from the standard ICP algorithm in that it has one more degree of freedom than the standard ICP, which may be why the Scale-ICP algorithm is more accurate.

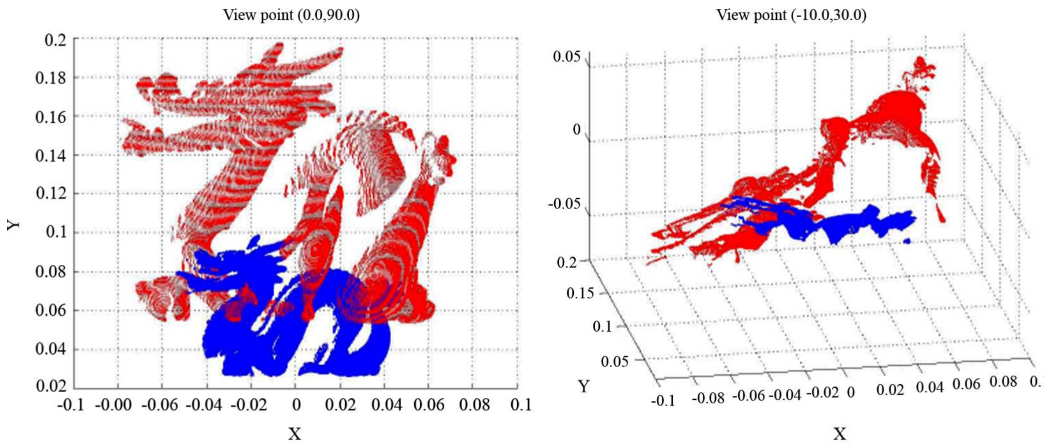

(a) View Point (0.0,90.0)
(b) View Point (-10.0,30.0)

Fig. 5. Original configuration of two data sets when $\mu = 0.5$.

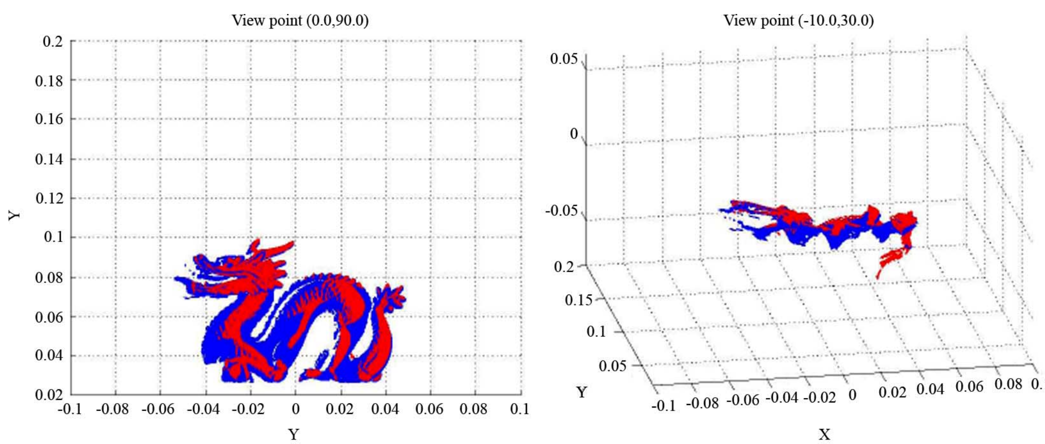

(a) View Point (0.0,90.0)
(b) View Point (-10.0,30.0)

Fig. 6. Configuration of two data sets after registration.

However, as same as all kinds of ICP algorithms, the algorithm we proposed is also local. Towards achieving a global optimum, we proposed a way of selection of initial registration. A point worth noticing is that the stretches existing in the data sets we considered in this paper are isotropic, which makes us able to use 1D scale factors to model the stretches. We have done our best to extend the Scale-ICP method to the anisotropic case, but unsuccessful. Indeed, in the anisotropic case, the noncommutativity between the scale matrix $S = \operatorname{diag}(s_1, s_2, s_3)$ and the rotation matrix R makes us unable to apply the SVD technique in solving the resulted optimization

$$\min e^k(R, S) = \sum_{i=1}^{m} \tilde{x}_i^T R^T \operatorname{Diag}(s_1^2, s_2^2, s_3^2) R\tilde{x}_i - 2\sum_{i=1}^{m} \tilde{z}_i^T \operatorname{Diag}(s_1, s_2, s_3) R\tilde{x}_i + \sum_{i=1}^{m} \tilde{z}_i^T \tilde{z}_i.$$

It seems to be not easy to solve such an optimization problem using the commonly used methods. However, it is really a very significant research issue.

References

[1] K. S. Arun, T. S. Huang, and S. D. Blostein, “Least square fitting of two 3-D point sets,” *IEEE Trans. Pattern Anal. Mach. Intell.*, vol. 9, no. 5, pp. 698–700, 1987.

[2] M. Á G. Ballester, X. Pennec, M. G. Linguraru, and N. Ayache, “Generalized image models and their application as statistical models of images,” *Med. Image Anal.*, vol. 8, pp. 361–369, 2004.

[3] P. J. Besl and N. D. McKay, “A method for registration of 3-D shapes,” *IEEE Trans. Pattern Anal. Mach. Intell.*, vol. 14, no. 2, pp. 239–256, 1992.

[4] Y. Chen and G. Medioni, “Object modeling by registration of multiple range image,” in *Proc. IEEE Conf. Robot. Autom.*, 1991, vol. 3, pp. 2724–2729.

[5] D. Chetverikov, D. Stepanov, and P. Krsek, “Robust Euclidean alignment of 3D point sets: The trimmed iterative closest point algorithm,” *Image and Vision Comput.*, vol. 23, pp. 299–309, 2005.

[6] E. Ezra, M. Sharir, and A. Efrat, “On the ICP algorithm,” in *Proc. the 22rd Ann. Symp. Computational Geometry*, 2006, pp. 95–104.

[7] J. Feldmar and N. Ayache, “Rigid, affine and locally affine registration of free-form surfaces,” *Int. J. Comput. Vision*, vol. 18, pp. 99–119, 1996.

[8] J. Feldmar, G. Malandain, J. Declerck, and N. Ayache, “Extension of the ICP algorithm to non-rigid intensity-based registration of 3D volumes,” in *Proc. Workshop Math. Methods Biomed. Image Anal.*, 1996, pp. 84–93.

[9] A. W. Fitzgibbon, “Robust registration of 2D and 3D point sets,” *Image and Vision Comput.*, vol. 21, pp. 1145–1153, 2003.

[10] H. Hügli and C. Schütz, “Geometric matching of 3D objects: Assessing the range of successful initial configurations,” in *Proc. IEEE Int. Conf. Recent Advances in 3D Digital Imaging and Modeling*, 1997, pp. 101–106.

[11] K. Kanatani, "Analysis of 3-D rotation fitting," *IEEE Trans. Pattern Anal. Mach. Intell.*, vol. 16, no. 5, pp. 543–549, 1994.
[12] S. Krishnan, P. Y. Lee, J. B. Moore, and S. Venkatasubramanian, "Global registration of multiple 3D point sets via optimization-on-a-manifold," in *Proc. Eurographics Symp. Geometry Processing*, 2005, pp. 1–11.
[13] Y. H. Liu, "Improving ICP with easy implementation for free-form surface matching," *Pattern Recogn.*, vol. 37, pp. 211–226, 2004.
[14] B. D. Lucas and T. Kanade, "An iterative image registration technique with an application to stereo vision," in *Proc. 7th Int. Joint Conf. Arti. Intell.*, 1981, pp. 121–130.
[15] X. Pennec and J. P. Thirion, "A framework for uncertainly and validation of 3D registration methods based on points and frames," *Int. J. Comput. Vision*, vol. 25, no. 3, pp. 203–229, 1997.
[16] B. M. Planitz, A. J. Maeder, and J. A. Williams, "The correspondence framework for 3D surface matching algorithm," *Computer Vision and Image Understanding*, vol. 97, pp. 347–383, 2005.
[17] H. Pottmann and M. Hofer, "Geometry of the squared distance function to curves and surface," in *Visualization and Mathematics III*, H. C. Hege and K. Polthier, Eds. New York: Springer, 2003, pp. 221–242.
[18] H. Pottmann, Q. X. Huang, Y. L. Yang, and S. M. Hu, "Geometry and convergence analysis of algorithms for registration of 3D shapes," *Int. J. Comput. Vision*, vol. 67, no. 3, pp. 277–296, 2006.
[19] S. Rusinkiewicz and M. Levoy, "Efficient variants of ICP algorithm," in *Proc. 3rd Int. Conf. 3D Digital Imaging and Modeling*, 2001, pp. 145–152.
[20] G. C. Sharp, S. W. Lee, and D. K. Wehe, "ICP registration using invariant features," *IEEE Trans. Pattern Anal. Mach. Intell.*, vol. 24, no. 1, pp. 90–102, 2002.
[21] S. Umeyama, "Least-squares estimation of transformation parameters between two point patterns," *IEEE Trans. Pattern Anal. Mach. Intell.*, vol. 13, no. 4, pp. 376–380, 1991.
[22] P. Yan and K. W. Bowyer, "A fast algorithm for ICP-based 3D shape biometrics," in *Proc. 4th IEEE Workshop on Autom. Identif. Adv. Technol.*, 2005, pp. 213–218.
[23] Z. Zhang, "Iterative point matching of free-from curves and surfaces," *Int. J. Comput. Vision*, vol. 13, no. 2, pp. 119–152, 1994.
[24] T. Zinßer, J. Schmidt, and H. Niemann, "A refined ICP algorithm for robust 3-D correspondence estimation," in *Proc. 2003 Int. Conf. Image Process.*, 2003, pp. 695–698.
[25] B. Zitová and J. Flusser, "Image registration methods: A survey," *Image and Vision Comput.*, vol. 21, pp. 977–1000, 2003.

Visual-Based Impedance Control of Out-of-Plane Cell Injection Systems

Haibo Huang, Dong Sun, James K. Mills, Wen J. Li, and Shuk Han Cheng

***Abstract*—In this paper, a vision-based impedance control algorithm is proposed to regulate the cell injection force, based on dynamic modeling conducted on a laboratory test-bed cell injection system. The injection force is initially calibrated to derive the relationship between the force and the cell deformation utilizing a cell membrane point-load model. To increase the success rate of injection, the injector is positioned out of the focal plane of the camera, used to obtain visual feedback for the injection process. In this out-of-plane injection process, the total cell membrane deformation is estimated, based on the $X-Y$ coordinate frame deformation of the cell, as measured with a microscope, and the known angle between the injector and the $X-Y$ plane. Further, a relationship between the injection force and the injector displacement of the cell membrane, as observed with the camera, is derived. Based on this visual force estimation scheme, an impedance control algorithm is developed. Experimental results of the proposed injection method are given which validate the approach.**

***Note to Practitioners*—In biological cell injection, the control of injection forces is important since excessive manipulation force may destroy the membrane or tissue of the biological cell, and lead to failure of the biomanipulation task. Although the injection force is a very important factor that affects the survivability of the injected cells, research on minimally invasive cell injection, based on understanding of the mechanical properties of the cellular membrane, are rare. To resolve this problem, a methodology is presented here to regulate cell injection forces using geometry of cell deformations and micro vision feedback. With the visually measured injection force applied to an injected cell, an impedance control strategy is then developed to regulate the cell injection force through the desired impedance. One advantage of using the impedance control in micromanipulation is that tiny forces exerted on the cell membrane can be reflected in the control system by adjusting the controller impedance coefficients.**

***Index Terms*—Biomanipulation, cell injection, impedance control, microrobotic system.**

I. Introduction

Since its invention during the first half of the last century, biological cell injection has been widely applied in gene injection [1], *in-vitro* fertilization (IVF) [2], intracytoplasmic sperm injection (ISCI) [3], and drug development [4]. Until very recently, however, existing research

Manuscript received August 13, 2007; revised November 22, 2007. First published May 12, 2009; current version published July 01, 2009. This paper was recommended for publication by Associate Editor M. Zhang and Editor D. Meldrum upon evaluation of the reviewers' comments. This work was supported by a grant from the Research Grants Council of the Hong Kong Special Administrative Region, China (Reference No. CityU 119705) and a grant from the City University of Hong Kong (Project No. 7002461).

H. B. Huang was with the Department of Manufacturing Engineering and Engineering Management, City University of Hong Kong, Kowloon, Hong Kong. He is now with the Department of Mechanical and Industrial Engineering, University of Toronto, Toronto, ON M5S 3G8, Canada (e-mail: hbhuang@mie.utoronto.ca).

D. Sun is with the Department of Manufacturing Engineering and Engineering Management, City University of Hong Kong, Kowloon, Hong Kong (e-mail: medsun@cityu.edu.hk).

J. K. Mills is with the Department of Mechanical and Industrial Engineering, University of Toronto, Toronto, ON M5S 3G8, Canada (e-mail: mills@mie.utoronto.ca).

W. J. Li is with the Centre for Micro and Nano Systems, Chinese University of Hong Kong, Shatin, NT, Hong Kong (e-mail: wen@acae.cuhk.edu.hk).

S. H. Cheng is with the Department of Biology and Chemistry, City University of Hong Kong, Kowloon, Hong Kong (e-mail: bhcheng@cityu.edu.hk).

Digital Object Identifier 10.1109/TASE.2008.2010013